UDC 629.7.058.54(043.2)/629.7.086:004.932.2 DOI: 10.15222/TKEA2014.1.23

I. G. PROKOPENKO, Dr.Sc., V. Iu. VOVK, I. P. OMELCHUK, Ph.D., Yu. D. CHIRKA, K. I. PROKOPENKO, Ph.D.

Ukraine, Kiev, National Aviation University
E-mail: prokop-igor@yandex.ru, vitalii.vovk@nau.edu.ua

LOCAL TRAJECTORY PARAMETERS ESTIMATION AND DETECTION OF MOVING TARGETS IN RAYLEIGH NOISE

The problem of detection of moving targets and estimation of local trajectory parameters based on the analysis of sensor data in the form of two-dimensional image is considered. In accordance with the target and sensor models, probability distribution of noise at the output of the detector is Rayleigh distribution, while probability distribution of signal is Rice distribution. Two trajectory parameters estimation techniques are considered: ordinary least squares and Hough transform. A detection stage based on the integration of an input signal along estimated trajectory is proposed. Statistical modeling was performed and detection characteristics were obtained.

Keywords: target detection, moving target, estimation, trajectory, track-before-detect, Rayleigh noise, Hough transform, least squares.

Moving targets detection and estimation of their trajectory parameters are the tasks of secondary stage of radar signal processing. Classical approaches to tracking and detection of moving low-snr (signal-to-noise ratio, **SNR**) targets are based on multi-survey analysis of radar data with thresholding procedure applied to it. In the case of rapid target detection tasks, it is necessary to reduce the number of surveys before decision about target presence can be made. Such rapid targets may produce on a radar image a few samples instead of one. In this case energy backscattered from the target is distributed along the entire trajectory, forming a track. This "blurring" effect causes the decreasing of SNR. For low-snr targets the threshold must be low (or even should be absent at all) to allow sufficient probability of target detection. A low threshold also gives a high rate of false detections which cause the tracker to form false tracks. In this case information about target trajectory may be very useful to provide an opportunity to integrate all backscattered from the target power along the entire trajectory.

The commonly used group of algorithms working with raw unthresholded data to estimate target state is known in literature as the track-before-detect (**TBD**) [1]. These methods are used when classical thresholding approaches are not suitable for tracking and detecting targets due to low SNR, typically stealthy military aircraft and cruise missiles, for which thresholding has an undesirable effect of disregarding potentially useful data [2].

Sensor image is often a highly nonlinear function of the target state (which describes kinematic and power parameters of the target). There are a number of methods to deal with this nonlinearity. First of all, such estimation techniques as the Viterbi algorithm [3] and the hidden Markov model (Baum-Welsh) filter or smoother [4] can be applied to the discretized state space, when nonlinearity is irrelevant due to such discretization. Such technique is used in several approaches to TBD, e.g. [5—7]. The main disadvantage of discretization of the state space leads to high computation and memory resource requirements.

To avoid the problems mentioned above, an alternative approach called "particle filtering" can be used to solve the nonlinear estimation task [2, 8]. This method (also called Sequential Monte Carlo) uses Monte Carlo techniques to solve the analytically intractable estimation integrals. It uses randomly placed samples instead of fixed samples as is the case for the discretized state space. Particle filtering has been used by a number of authors for TBD, e.g. [9—11]. In many cases it is possible to achieve close or even similar estimation performance for lower cost by using less sampling points than would be required for a discrete grid.

An alternative approach to estimation of the target state is called the histogram probabilistic multi-hypothesis tracking (**PMHT**) algorithm [12]. In this method, a parametric representation of the target state pdf is used rather than a numerical one. This makes it possible to reduce the computational load of the algorithm. The main idea of maximum likelihood probabilistic data association (**PDA**) is to reduce the threshold to a low level and then apply a grid-based state model for estimation [13, 14] rather than using the whole

sensor image. The association of the high number of measurements is handled using PDA.

In addition to estimating the target state, the TBD algorithm needs to detect the presence or absence of targets. One method to do this is to extend the state space by including target presence state. In this case, null-presence state will correspond to the case when there is no target [9, 15]. A target is detected when any state other than the null state has the highest probability. Another closely related concept is to use a separate Markov chain to describe the target presence state as originally introduced for PDA in [16]. This approach has been used for the particle filter [10] and a generalized version was applied to the PMHT [17]. Comparison of detection performance for TBD algorithms mentioned above has been done by Davey, et al. [18].

Many of the articles mentioned above deal with radar data in the form of a two-dimensional image. The x and y axes correspond to range-bearing subspace of a global range-bearing-elevation-doppler measuring hypercube, or to linear space coordinates, which are obtained from these measurements. It is usually assumed that equal size of resolution bins (cells) may be feasible in case when space being studied is a small part of the observed sector and is far enough from the sensor.

A sequence of radar images is usually processed before the decision about target presence or absence can be made in TBD approaches. A target is usually a point scatterer which produces a blurred spot on the radar image (**Fig. 1**), moving from frame to frame according to the kinematic parameters of the target.

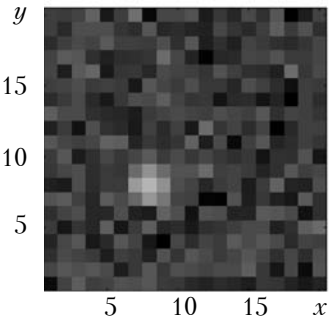

Fig. 1. Example of a radar image in some TBD applications [11]

In this paper we describe the approach, which has two main distinctions from the methods mentioned above. Firstly, to decrease computational efforts, we try to avoid using any grid-based algorithms, either uniform or non-uniform (as in particle filtering). For the same reason we do not estimate the target state pdf. Secondly, our method can be applied to analyze a radar image, which may contain not just a single sample, but a track of the moving target. This fact gives additional information which can be used to reduce a number of analyzed radar images before decision about target presence can be made. Such images can be formed from a sequence of radar plots in case of slow moving targets, or even a single radar plot in case of rapid moving targets ("rapid" compared with the radar image forming time). Here several assumptions are made: 1) the target is a point scatterer; 2) the target has enough speed to produce track while the radar image (frame) is being formed; 3) the trajectory of the target is close to linear; 4) all resolution cells (bins) are of equal size. This can be relevant in case of small radar target (e.g. cruise missile) tracked by phased-array or multiple beams systems with wideband signal (e.g. MIMO radars with pseudo-noise signals or systems with frequency modulated pulse compression). The similar radar images can be obtained by observing ionized trails in atmosphere produced by meteors in radar meteor detection systems [19]. However, in this case we deal with a linearly distributed target. Another interpretation of the xy-plane could be a projection of space volume onto the sensor in optical or infrared systems (e.g. forward looking infrared, **FLIR** [20]). Such systems are used in some cases when a high resolution is needed (e.g. for detection of meteors or fast cruise missiles) [21]. Hereinafter we will assume that the target is a fast moving point radar object.

The proposed algorithm contains two main stages [22]. At the first stage geometric parameters of a potential trajectory should be estimated. There are two commonly used methods to perform such estimation: ordinary least squares technique [23] and Hough transform [24]. At the second stage a decision about target presence is made by simple detection technique based on the integration along the track of a power backscattered from the target. This algorithm can also be used for more accurate forming of proposed distributions in particle filter TBD approaches, or as initiation procedure for complex trajectory detection by analysis of its small linear part.

Target, signal and sensor models

Target model

As it was mentioned earlier we assume the target to be a rapid point-scattering object. We take into account two models of target moving: linear and non-linear (parabolic). The linear target moving model can be described in Cartesian x-y-plane in the form $\rho = x(t)\cos\theta + y(t)\sin\theta$ or, which is equal to $\rho = x(t)\sin\varphi + y(t)\cos\varphi$ (see **Fig. 2**), where ρ is the distance from the origin to a straight line, to which trajectory belongs; θ is the anticlockwise angle between the x-axis and the perpendicular from the origin to the straight line; $\varphi = -(\theta - \pi/2)$;

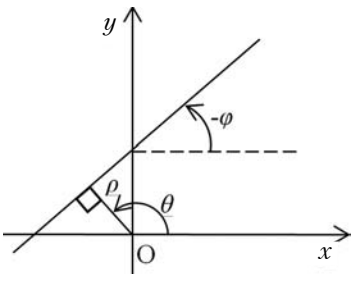

Fig. 2. Geometric representation of a straight line

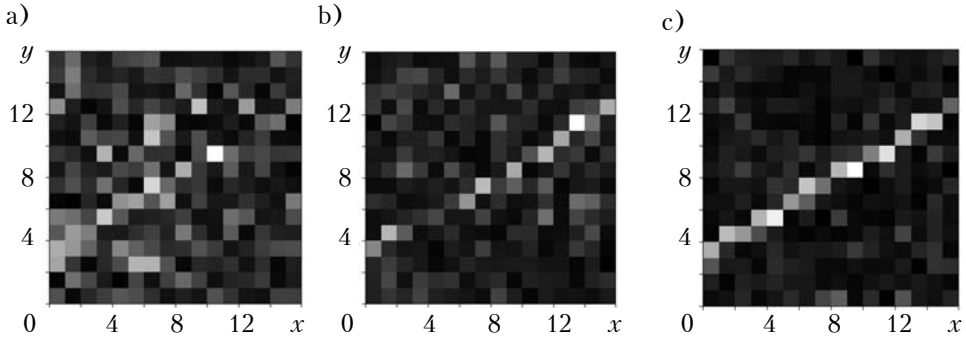

Fig. 3. Images with simulated linear tracks of moving target for signal-to-noise ratio equals 4 dB (*a*), 7 dB (*b*) and 10 dB (*c*)

x and y are the space coordinates; t is time (either continuous or discrete).

The parabolic target moving model is described by the equation $y(t) = a_2x^2 + a_1x + a_0$. We should note that such representation does not take into account the possible rotations of the parabolic trajectory.

Signal model

The signal at the input of the sensor is a sequence of radio pulses with constant carrier frequency ω, random phase φ and constant amplitude v_S. The noise is an additive Gaussian random process. Thus, along the trajectory, the signal-noise model is

$$S = v_S \cos(\omega t + \varphi) + w, \quad (1a)$$

and outside the trajectory, the model is

$$S = w. \quad (1b)$$

Here $w \sim N(0,\sigma_N)$, σ_N is a standard deviation of noise; $N(m,\sigma)$ denotes Gaussian distribution with mean m and standard deviation σ.

Sensor model

The analysed image is a grayscale image formed from the output of the amplitude detector. According to (1), values of each pixel (sample) of the image are distributed with Rice distribution, if such sample belongs to the trajectory of the target [25, p. 19]:

$$z_{x,y} = \frac{w_{x,y}}{\sigma_N^2} \exp\left(\frac{-(w_{x,y}^2 + v_S^2)}{2\sigma_N^2}\right) I_0\left(\frac{w_{x,y} v_S}{\sigma_N^2}\right), \quad (2a)$$

and with Rayleigh distribution, if it does not:

$$z_{x,y} = \frac{w_{x,y}}{\sigma_N^2} \exp\left(\frac{-(w_{x,y}^2)}{2\sigma_N^2}\right), \quad (2b)$$

where $I_0(\cdot)$ is the modified Bessel function of zero order; x and y are coordinates of the sample.

Some examples of images which correspond to the model described by (2) are presented in **Fig. 3** (hereinafter the measure units for x and y axes will be the same nominal units, the size of image pixel corresponds to the size of the resolution cell).

Selection of important samples

The trajectory parameters estimation procedure consists of two subtasks. At first we need to select a set of samples (hereinafter "important samples") from the source image, which will be used later for estimation of the trajectory parameters. Then, the parameters of the trajectory must be estimated in some way. We shall consider Hough transform and ordinary least squares techniques to do this. Both techniques in a 2D-image case require set of samples' coordinates as the input. We consider a several methods to select such samples, based on order statistics.

The first method involves the independent applying of two Boolean masks to the original image. Both masks are of the same size as the original image. The first mask is formed in the following way. For every row of it we set "true" in the bin, which holds the maximum value in the corresponding row of the source image (*R*-mask) and "false"

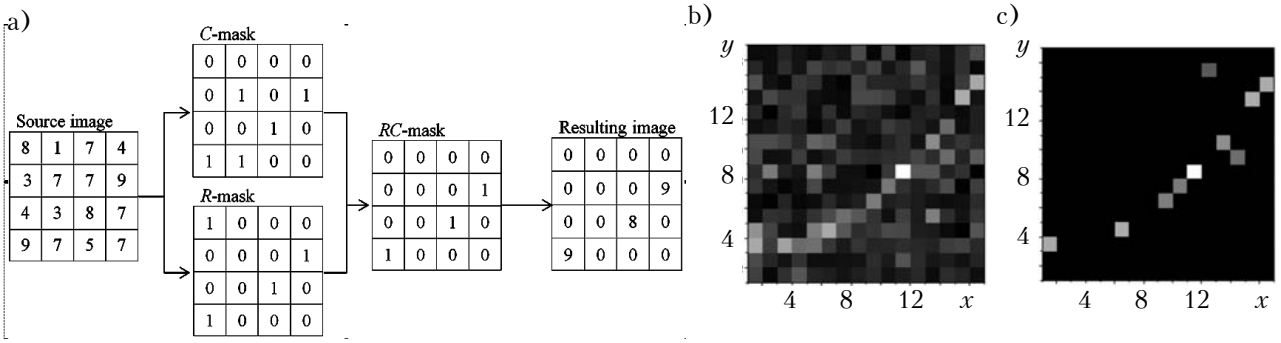

Fig. 4. Procedure for selecting important samples (RC-mask) (*a*) and example of its application: *b* — source image; *c* — resulting image

elsewhere. The second mask is formed in the same way, but for columns (C-mask). These masks are then independently applied to the source image. Thus, we obtain two sets of important samples for further analysis. The second method is based on applying to the source image the result of a conjunction of R- and C-masks RC = R∧C (**Fig. 4**).

The third method assumes additional use of two binary masks formed in the same way as *R*-mask and C-mask but for diagonal (D-mask) and cross-diagonal (CD-mask) elements. Thus, the resulting mask RCD = (R∧C) ∨ (D∧CD).

The normalized power properties for different sample selection techniques are shown in **Fig. 5** (P_{SEL} is the power that corresponds to selected important samples; P_{SIG} is the full power backscattered from target power; P_{SP} is the power backscattered from the target power that corresponds to selected important samples). These plots were obtained as a result of computer modeling with number of simulations N=2,000 and image size 16×16 pixels (all simulated tracks were built in the way they crossed the center of the image). In Fig. 5, *a* the power that corresponds to selected important samples normalized to full signal power (full power backscattered from target) is shown. It can be clearly seen that in low-snr region important samples mainly correspond to noise. Fig. 5, *b* shows that for all proposed techniques the amount of used signal power (the backscattered power that corresponds to the true trajectory) is increased with the increase of SNR, but RC technique rejects the half of useful data. At the same time, as it can be seen from Fig 5, *c*, RC technique shows the lowest level of noise samples power among other sample selection techniques. This is important for trajectory parameters estimation procedures, because, due to low order of trajectory nonlinearity, its parameters still can be estimated by small number of important samples (2 or 3). Due to this fact, it is better to lose some useful information at this step, but reduce more noise samples. The average number of selected noise samples for different sample selection technique in case when there is no actual track presented in the radar plot of size $M \times M$ is shown in **Table 1**.

We should note that such approach cannot be applied in case of two or more closely-spaced targets, because of missing and mixing data from such targets.

To additionally reduce the number of noise samples being selected, an additional clearing procedure

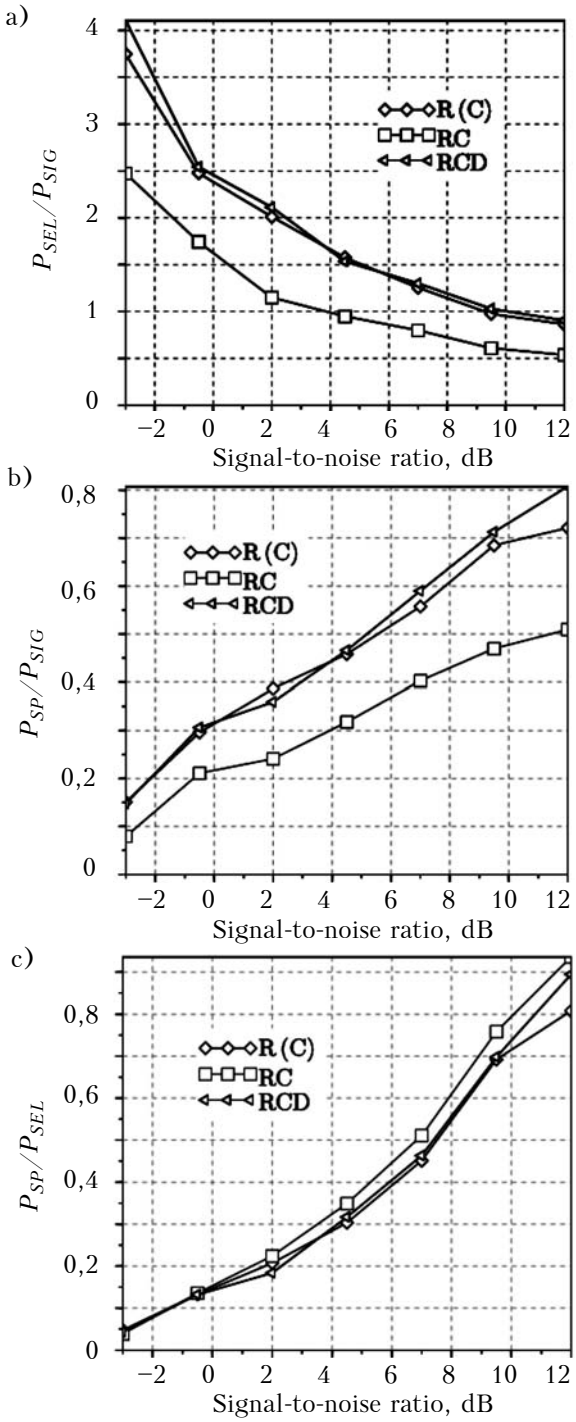

Fig. 5. Normalized power properties for different sample selection techniques

Table 1

Average number of selected samples for different sample selection techniques

Sample selection technique	R(C)	RC	RCD
Average number of selected samples	M	$\frac{M^2}{2(M-1)}$	$\sum_{i=1}^{M}\sum_{j=1}^{M}\frac{1}{k_{i,j}+l_{i,j}-1}$, $k_{i,j}=\begin{cases}M-i+j, \text{if } i>j,\\ M-j+i, \text{otherwise};\end{cases}$ $l_{i,j}=\begin{cases}i+j-1, \text{if } M-j+1>i,\\ 2M-i-j+1, \text{otherwise}.\end{cases}$

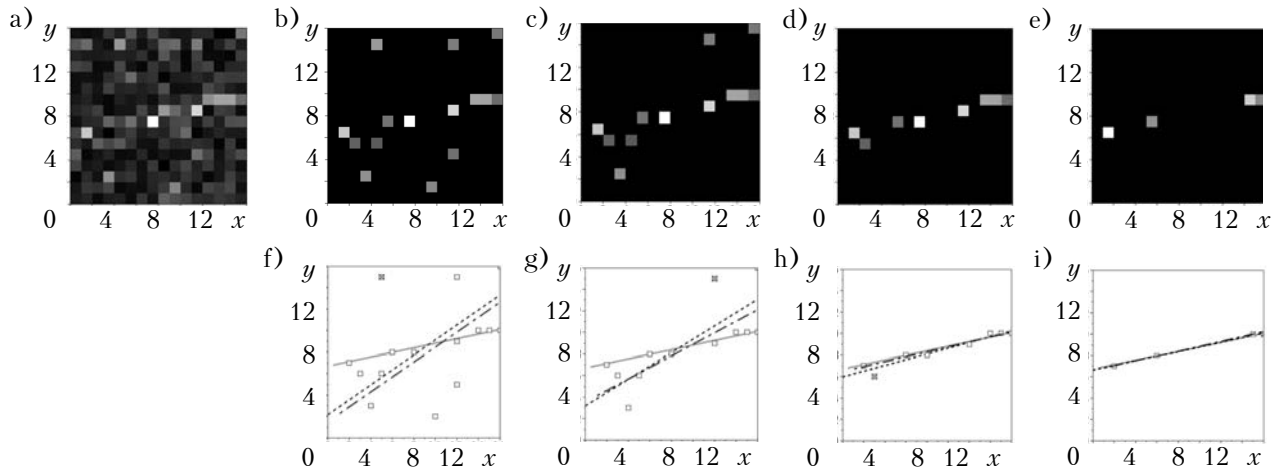

Fig. 6. Clearing procedure for linear trajectory (SNR = 5 dB):
a — source image; *b*, *c*, *d*, *e* — important samples at steps *1*, *4*, *8* and *12*; *f*, *g*, *h*, *i* — true trajectory (solid), estimated trajectory before clearing step (dash), estimated trajectory after clearing step (dash-dot) at the same steps; the crossed sample is the sample which is removed at the current clearing step

can be introduced in case of linear trajectories. This procedure contains following steps:

1. Select important samples from the source image.
2. For every important sample estimate the trajectory parameters without considering this sample, and evaluate the deviation of other samples around estimated trajectory.
3. Remove the sample which, if not taken into account, minimizes deviation.
4. Go to step 1 until stop-condition is not met.

This stop-condition could be the number of important samples left (at least two samples must be left to estimate linear trajectory parameters) or the deviation of the samples is less than predefined threshold. The example of usage of such procedure is shown in **Fig. 6**.

Of course, in some cases, especially for low-snr signals, this procedure can fail. But, as shown below, in general, it gives a gain in quality of trajectory parameters estimation and, as a result, in detection performance.

Estimation of the geometric parameters of the trajectory

Once important samples have been selected, trajectory parameters can be estimated. There is a well-described in literature technique, called Hough transform **(HT)** [26, 27], commonly used in image processing for estimating geometric parameters of parametric curves [24]. Nowadays it is widely used in different image processing tasks, from radar and sonar signal processing [28] to object recognition tasks and machine vision [29]. The main idea of Hough transform technique is to map points from the local coordinate space to curve's parameters space and find a maximum in this new space. This maximum will correspond to the most likely parameters of the curve. To do this, the so called accumulator array is built by discretization the space of parameters with steps Δ_i, where $i = 1...N$, and N is the number of parameters of the curve. Then, for every important sample we look through possible parameters of the curve which satisfies curve equation, and add one (or some other value corresponding to the weight of a sample) to the corresponding bin of the accumulator. This can be illustrated in **Fig. 7** for the case of two straight lines (Fig. 7, *a*), which can be described in Cartesian xy-plane in the form $\rho = x\cdot\cos\theta + y\cdot\sin\theta$ [24] (see Fig. 2). In Fig. 7, ρ, x and y are measured in the same nominal units, θ is measured in degrees.

An alternative well-known technique for estimating parameters of parametric curves is ordinary least squares **(OLS)** [23]:

$$\hat{\theta} = \arg\min_{\theta}(S^T K S), \qquad (3)$$

where $S = [s_1,...,s_L]$;
T is vector of errors;
s_j is the error or the "distance" between the model and the j^{th} data point, $s_j = f(x_j, y_j, \theta)$;
K is covariance matrix;
θ is vector of model (curve) parameters.

In case of straight lines in some two-dimensional space without any preferred directions, (3) can be rewritten as:

$$\hat{\theta} = [\hat{\rho}, \hat{\varphi}] =$$

$$= \arg\min_{\rho,\varphi}\left\{\frac{1}{n}\sum_{i=1}^{n}(x_i\sin\varphi + y_i\cos\varphi - \rho)^2. \qquad (4)\right.$$

Denoting

$$e = \frac{1}{n}\sum_{i=1}^{n}(x_i\sin\varphi + y_i\cos\varphi - \rho)^2, \qquad (5)$$

where ρ can be treated as the "distance" from the origin to the line;
$-\varphi$ is the angle between the Ox axis and the straight (Fig. 2);
x_i, y_i are coordinates of the i^{th} sample;
n is the number of important samples.

and using (4) OLS for fitting data by a straight line model can be written as follows:

$$\begin{cases} \dfrac{\partial e}{\partial \rho} = -\dfrac{2}{n}\sum\limits_{i=1}^{n}(x_i \sin\varphi + y_i \cos\varphi - \rho) = 0, \\ \dfrac{\partial e}{\partial \varphi} = \dfrac{2}{n}\sum\limits_{i=1}^{n}(x_i \sin\varphi + y_i \cos\varphi - \rho) \times \\ \qquad \times (x_i \cos\varphi + y_i \sin\varphi) = 0, \end{cases} \quad (6)$$

whence we obtain

$$\begin{cases} \rho = \sin\varphi \cdot E[x] + \cos\varphi \cdot E[y], \\ (4A^2 + B^2)p^2 - (4A^2 + B^2)p + A^2 = 0, \end{cases} \quad (7)$$

where $E[\cdot]$ is the mean value of the expression in brackets;

$p = \cos^2\rho$;

$A = E[xy] - E[x]\cdot E[y]$;

$B = (E[y^2] - E^2[y]) - (E[x^2] - E^2[x])$.

The sign of cosφ can be obtained as follows. If $\sin\varphi = \sqrt{1-p} \geq 0$, then

$$\begin{cases} \cos\varphi = \sqrt{p}, \text{if } (\sqrt{p} \geq \sin\varphi \wedge A \geq 0 \wedge B \geq 0) \vee \\ \qquad \vee (\sqrt{p} \geq \sin\varphi \wedge A < 0 \wedge B < 0) \vee \\ \qquad \vee (\sqrt{p} < \sin\varphi \wedge A \geq 0 \wedge B < 0) \vee \\ \qquad \vee (\sqrt{p} < \sin\varphi \wedge A < 0 \wedge B \geq 0), \\ \cos\varphi = \sqrt{p}, \text{otherwise}, \end{cases} \quad (8)$$

while ρ can be either positive or negative.

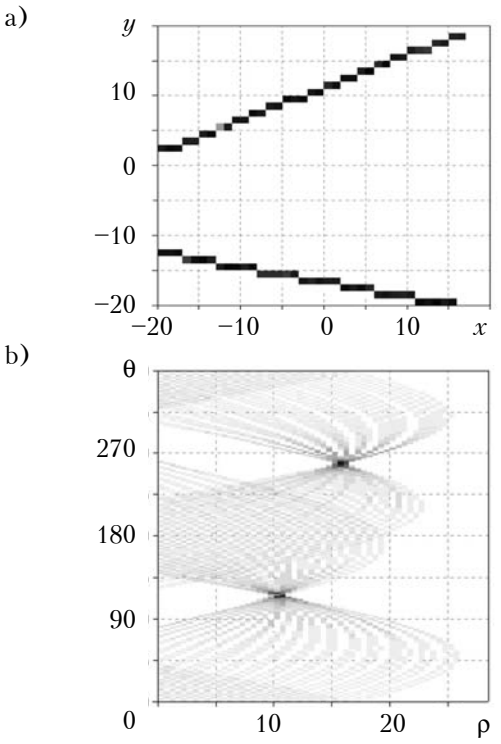

Fig. 7. Source image, containing two straight lines (*a*) and parametric space with two maximums (*b*)

To determine which of the roots of the quadratic equation in (7) minimizes (5), the second-order differential must be analyzed. Roots which minimize (5) must satisfy the following conditions:

$$\Delta = \begin{vmatrix} A & B \\ B & C \end{vmatrix} = AC - B^2 > 0 \text{ and } A > 0, \quad (9)$$

where

$$A = \frac{\partial^2 e}{\partial \rho^2} = 2; B = \frac{\partial^2 e}{\partial \rho \partial \varphi} = -\frac{2}{n}\sum_{i=1}^{n}(x_i \cos\varphi - y_i \sin\varphi);$$

$$C = \frac{\partial^2 e}{\partial \varphi^2} = \frac{2}{n}\sum_{i=1}^{n}[(x_i^2 - y_i^2)(\cos^2\varphi - \sin^2\varphi) + \rho(x_i \sin\varphi + y_i \cos\varphi)].$$

If Δ=0 then minimum of (5) can be found by a small variation of estimated parameters and analyzing the behavior of (5).

For parabolic trajectories OLS can be simply written as

$$\hat{A} = \arg\min_{a_2, a_1, a_0}\{e\},$$

where $e = \frac{1}{n}\sum_{i=1}^{n}(y_i - a_2 x_i^2 + a_1 x_i + a_0)^2$,

or, as a system of linear equations:

$$\begin{cases} \dfrac{\partial e}{\partial a_2} = \dfrac{2}{n}\sum\limits_{i=1}^{n}(a_2 x_i^2 + a_1 x_i + a_0 - y_i) x_i^2 = 0, \\ \dfrac{\partial e}{\partial a_1} = \dfrac{2}{n}\sum\limits_{i=1}^{n}(a_2 x_i^2 + a_1 x_i + a_0 - y_i) x_i = 0, \\ \dfrac{\partial e}{\partial a_0} = \dfrac{2}{n}\sum\limits_{i=1}^{n}(a_2 x_i^2 + a_1 x_i + a_0 - y_i) = 0. \end{cases} \quad (10)$$

Thus, the parameters of parabolic trajectory form the vector $\hat{A} = [a_2, a_1, a_0]$ which satisfies (10). It should be noted, that such technique does not take into account possible rotation of parabolic trajectory.

Detection step

To make a decision about the presence of a target in the analyzed image, an integration of values over obtained trajectory is performed. The integration is carried out over a certain band around the estimated trajectory (**Fig. 8**). Thus, decision rule for target detection is $S > V_D$, where

$$S = \frac{1}{m}\sum_{i=1}^{m} w_i^2, \quad (11)$$

V_D is the decision threshold, defined for previously specified probability of false alarm;

w_i is the value of the i^{th} sample within the integration strip;

m is the number of samples within integration strip.

In this paper we consider simple parametric detection procedure, which does not provide a constant probability of false alarms with change of noise power. To provide constant false alarm

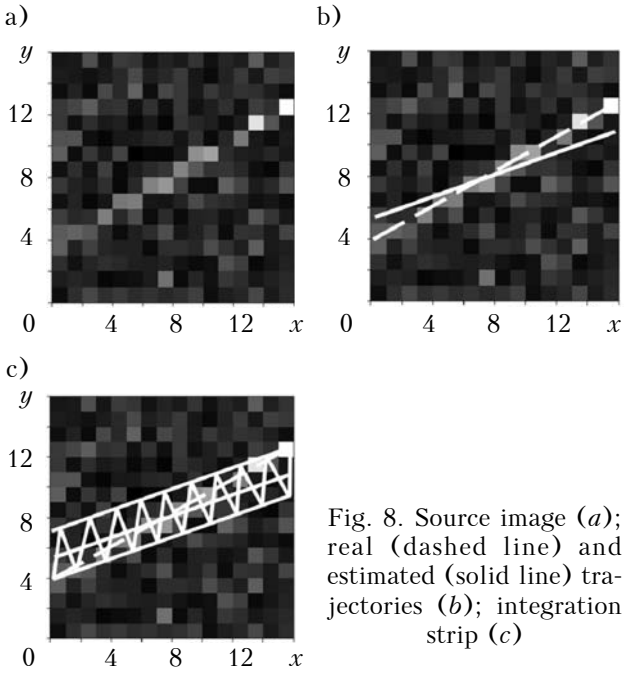

Fig. 8. Source image (*a*); real (dashed line) and estimated (solid line) trajectories (*b*); integration strip (*c*)

ratio additional procedure for estimation of the noise power should be introduced, and detection threshold for statistics (11) should be changed depending on such estimation.

Since the result of a detection procedure depends on the estimated parameters, some arrangements can be made to improve the accuracy of the estimation, for example, preprocessing of the source image by smoothing. The effect of preprocessing in case of Gaussian kernel smoothing and mean-smoothing will be shown in the next section.

Statistical modeling and simulation results

To obtain detection characteristics 5,000 simulations for each value of SNR were made. Dimensions of test images are 16×16 pixels. Integration strip width is set to 2. Probability of false alarms is set to 0,01. According to the signal and sensor models, signal-to-noise ratio in each bin of the image is defined as $10\log_{10}(v_S^2/(2\sigma_N^2))$, where v_S is the amplitude of the modeled signal; σ_N^2 is the noise variance. All linear tracks were modeled in the way they crossed the center of the image.

In **Fig. 9** detection characteristics and estimation errors are shown for different sample selection techniques (discussed above): by independently applying R- and C-masks and finding a maximum of (11) among two sets of samples (RCM); by applying RC-mask (RC); by applying RCD-mask (RCD). Ideal detection characteristic in case of known trajectory parameters is also shown for comparison. OLS technique was used for trajectory parameters estimation.

The unit of y-axis for RMSE of $\hat{\rho}$ is one resolution cell. The unit of y-axis for RMSE of $\hat{\varphi}$ is one radian. A "hat" symbol means that these values are

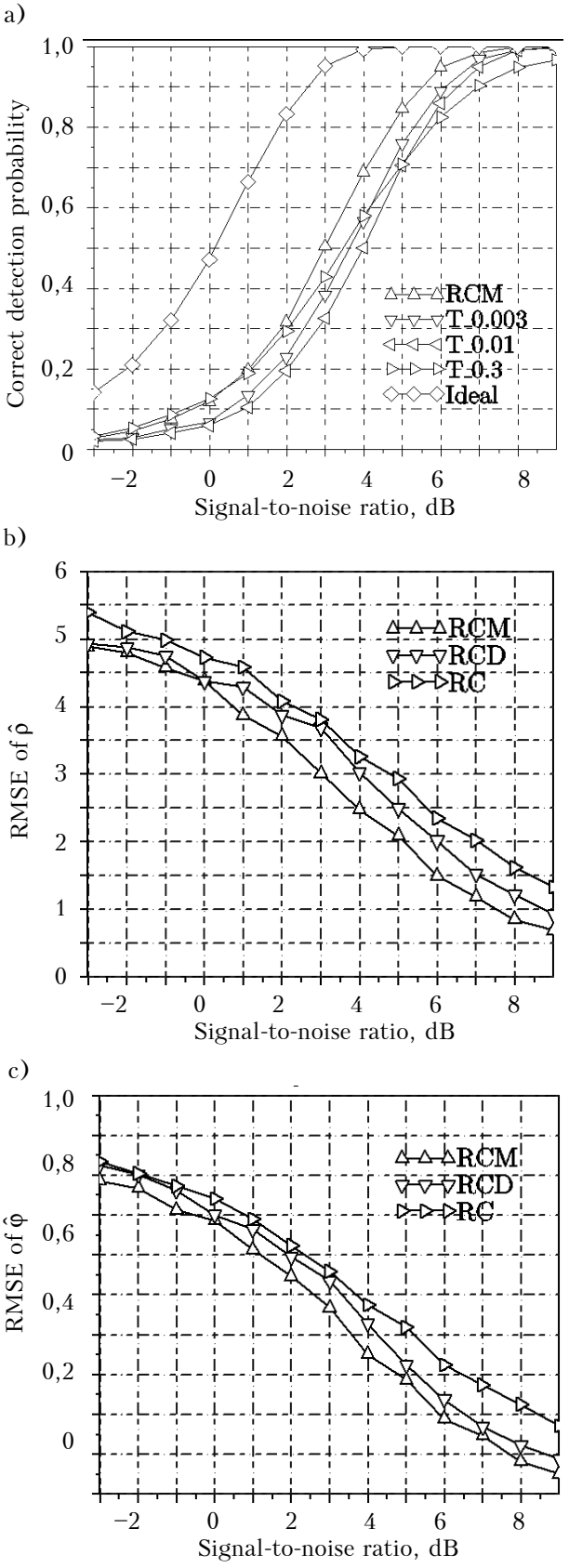

Fig. 9. Detection characteristics (*a*) and parameters estimation errors (*b*, *c*) for different sample selection techniques

estimates of the true parameters. For comparison, in **Fig. 10** the same characteristics are shown for the case when thresholding is applied as a sample selection technique with probabilities of exceeding the threshold for noise equal to 0.003, 0.01 and 0.3 (T_0.003, T_0.01 and T_0.3 respectively). OLS technique was used for trajectory parameters estimation.

Fig. 11 shows the detection characteristics and estimation errors for different techniques of estimating trajectory parameters: OLS and HT. For HT the next initialization parameters were used: step by "distance" $\Delta\rho$=1 resolution cell (rc), step by angle $\Delta\varphi$=1°.

Fig. 12 shows the influence of the following initialization parameters for the HT: $\Delta\rho$=1 rc, $\Delta\varphi$=1° (HT_1); $\Delta\rho$=1 rc, $\Delta\varphi$=2° (HT_2); $\Delta\rho$=2 rc, $\Delta\varphi$=1° (HT_3); $\Delta\rho$=0,5 rc, $\Delta\varphi$=0,5 deg (HT_4). RCM-technique is used for sample selection.

In **Fig. 13** the effects of preprocessing smoothing step in case of Gaussian kernel smoothing and mean smoothing are shown. The radius of smoothing is 1 cell (i.e. the size of smoothing region for each pixel is 3×3), parameter of Gaussian kernel was set to σ_{SM}=1,5. RCM is used for sample selection, OLS is used for parameters estimation. It can be seen that Gaussian kernel smoothing gives a gain on the correct detection probability as well as on the accuracy of trajectory parameters estimation.

In **Fig. 14** the effect of applying the clearing step for reducing the number of false important samples is shown. OLS technique was used for trajectory parameters estimation. The next complex stop-condition was used: either number of samples is less than 3 or their variance around estimated trajectory is less than 1.

Fig. 15 shows detection characteristics in case of parabolic trajectory model. It can be seen, that in this case the detection algorithm in general shows worse performance in comparison with the linear trajectory case. In some cases, as for the one in **Fig. 16**, *a*, the use of a linear model for integration (PT-LE_1) instead of a parabolic model (PT-PE_1) may give better detection performance. But in most cases, as in Fig. 16, *b*, the parabolic model should be used (PT PE_2). In general, linear trajectory model is more robust to noise samples than second or higher orders models.

In reality, the trajectory of moving target can often be approximated by a sequence of linear paths. This fact allows us to use proposed algorithm to detect such paths, which can be then joined into a full target trajectory. As an example, an application of the proposed algorithm for tracking moving targets is shown in Fig. **17**. In this figure a sequence of simulated radar plots as well as results of target detection for each plot are shown.

The size of a radar plot is 256×256 pixels. Each plot is divided into subplots of 16×16 pixels which are used for further analysis.

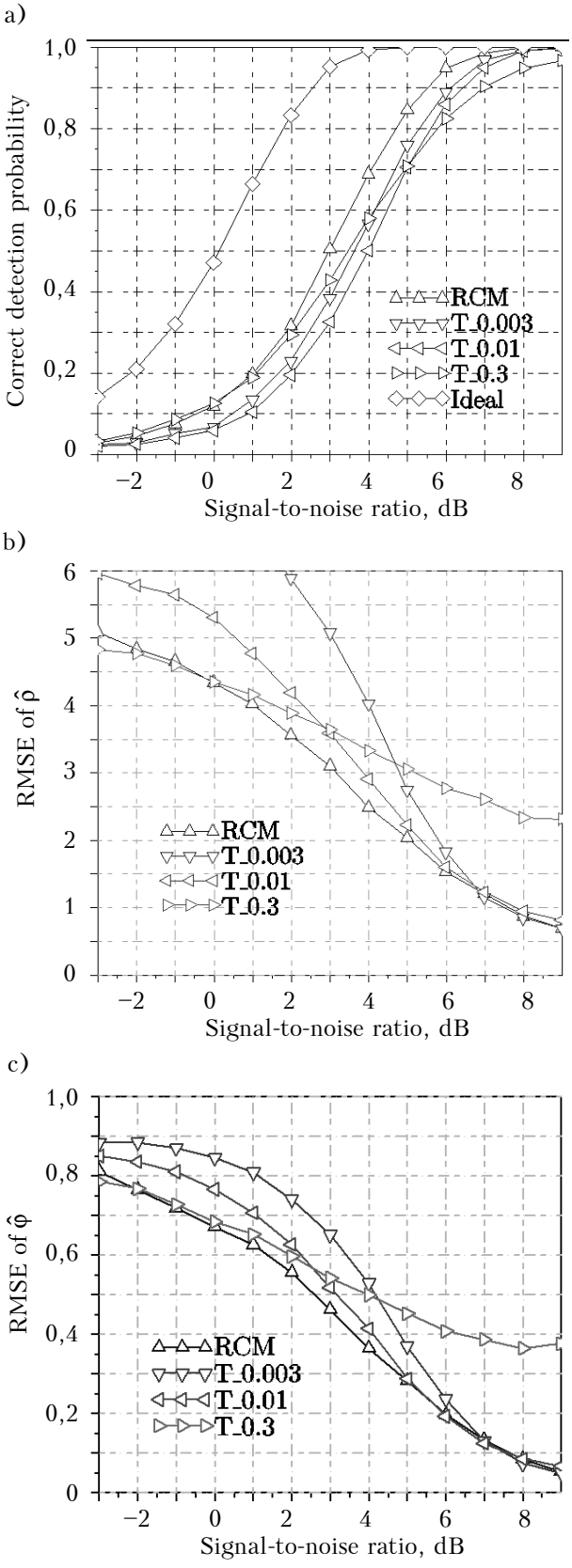

Fig. 10. Detection characteristics (*a*) and parameters estimation errors (*b*, *c*) for thresholding procedure as an important samples selection technique (RCM is shown for comparison)

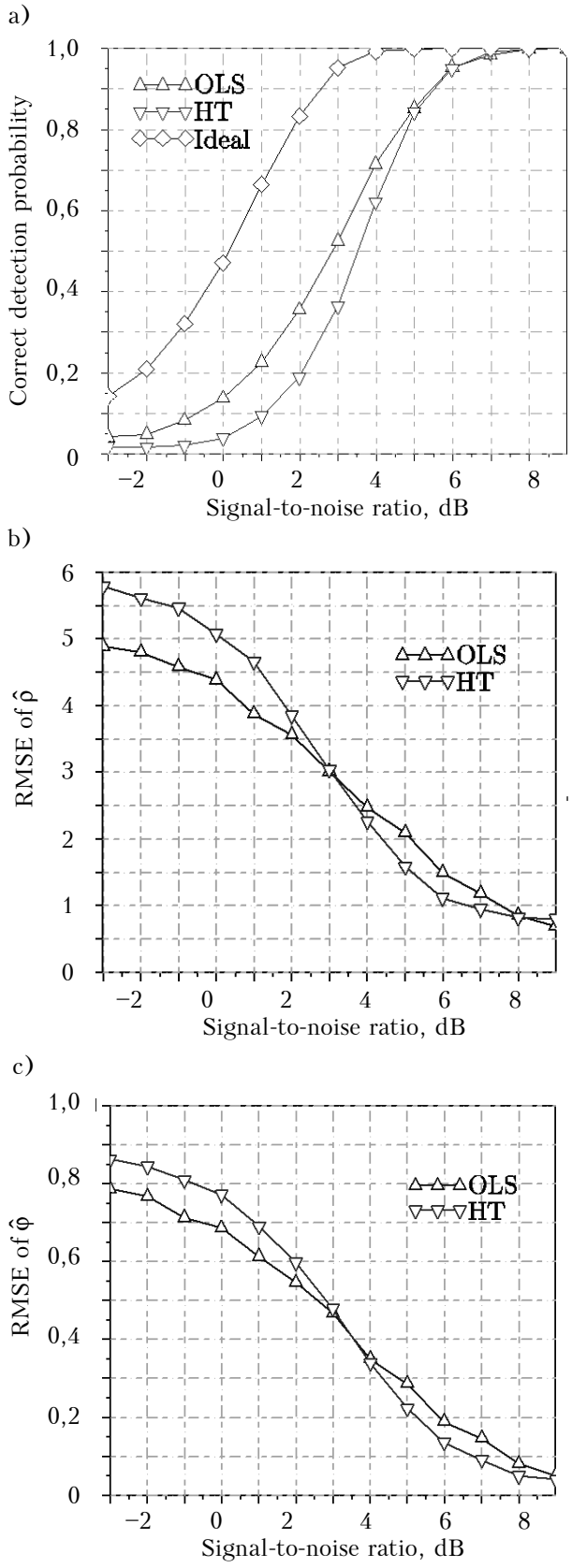

Fig. 11. Detection characteristics (*a*) and parameters estimation errors (*b*, *c*) for OLS and HT techniques of estimating the trajectory parameters

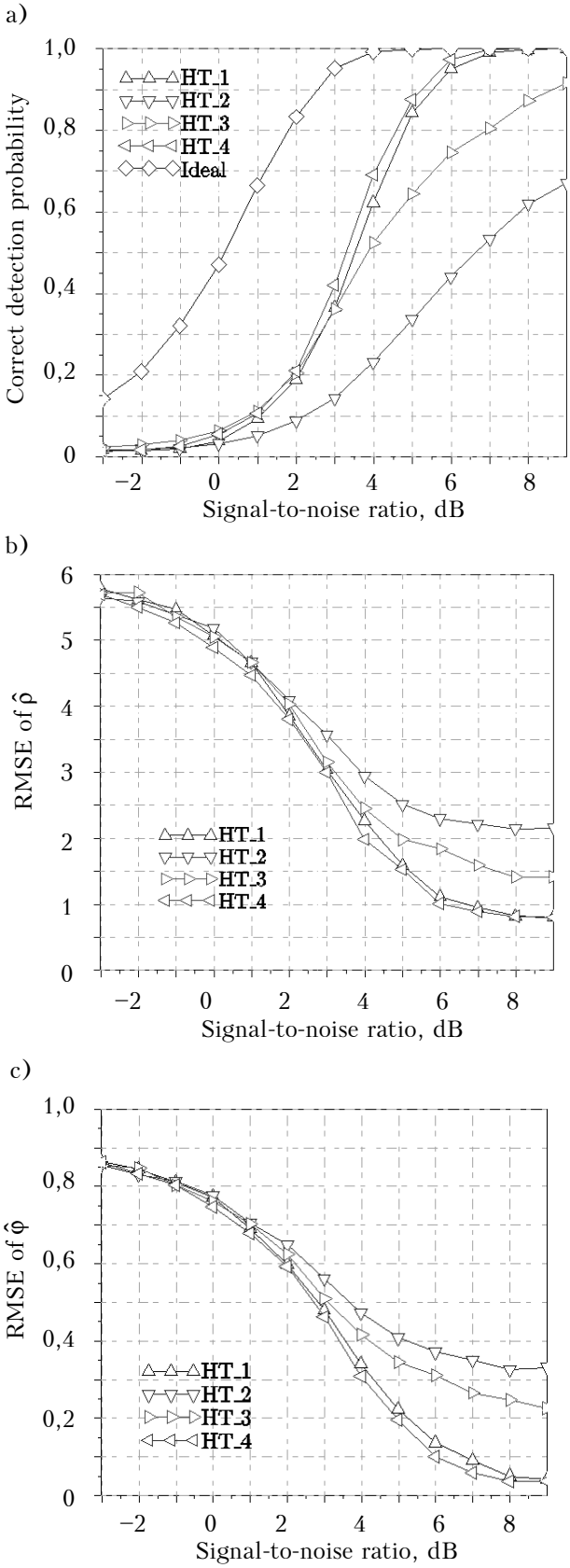

Fig. 12. The influence of initialization parameters of the HT on detection characteristics (*a*) and parameters estimation errors (*b*, *c*)

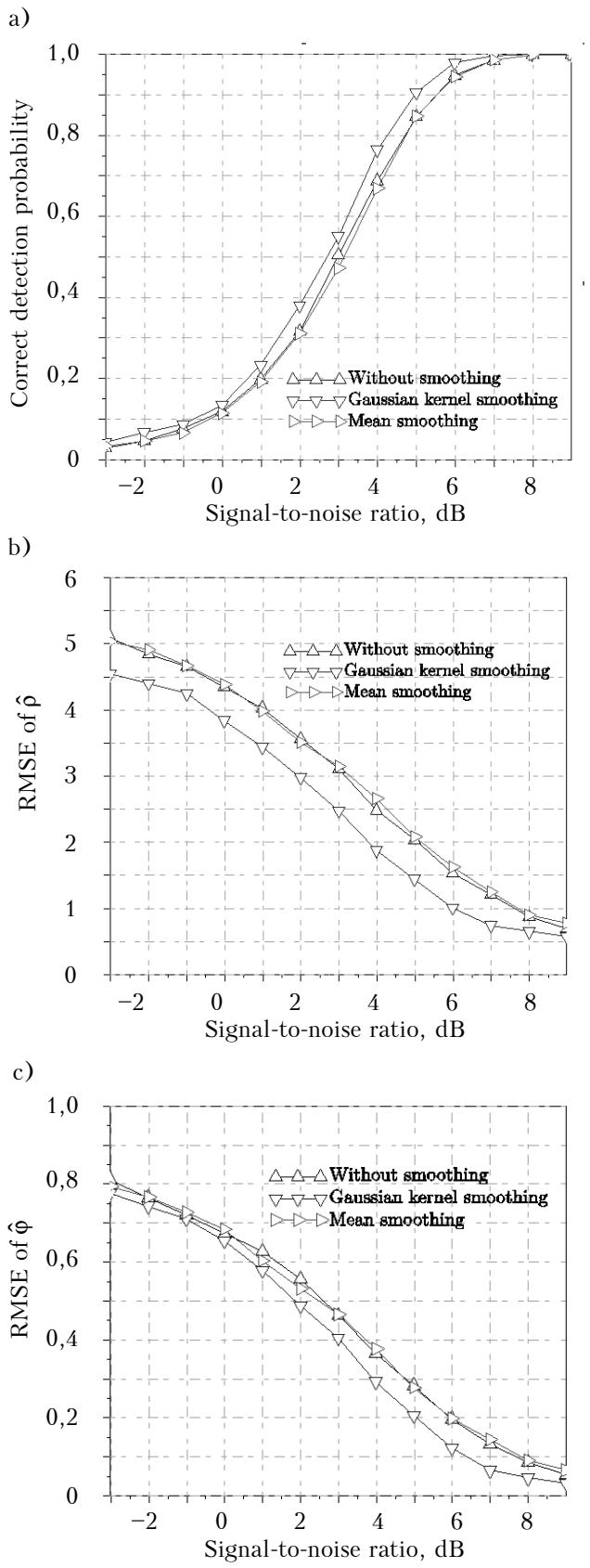

Fig. 13. Detection characteristics (*a*) and estimation errors (*b*, *c*) for different smoothing techniques

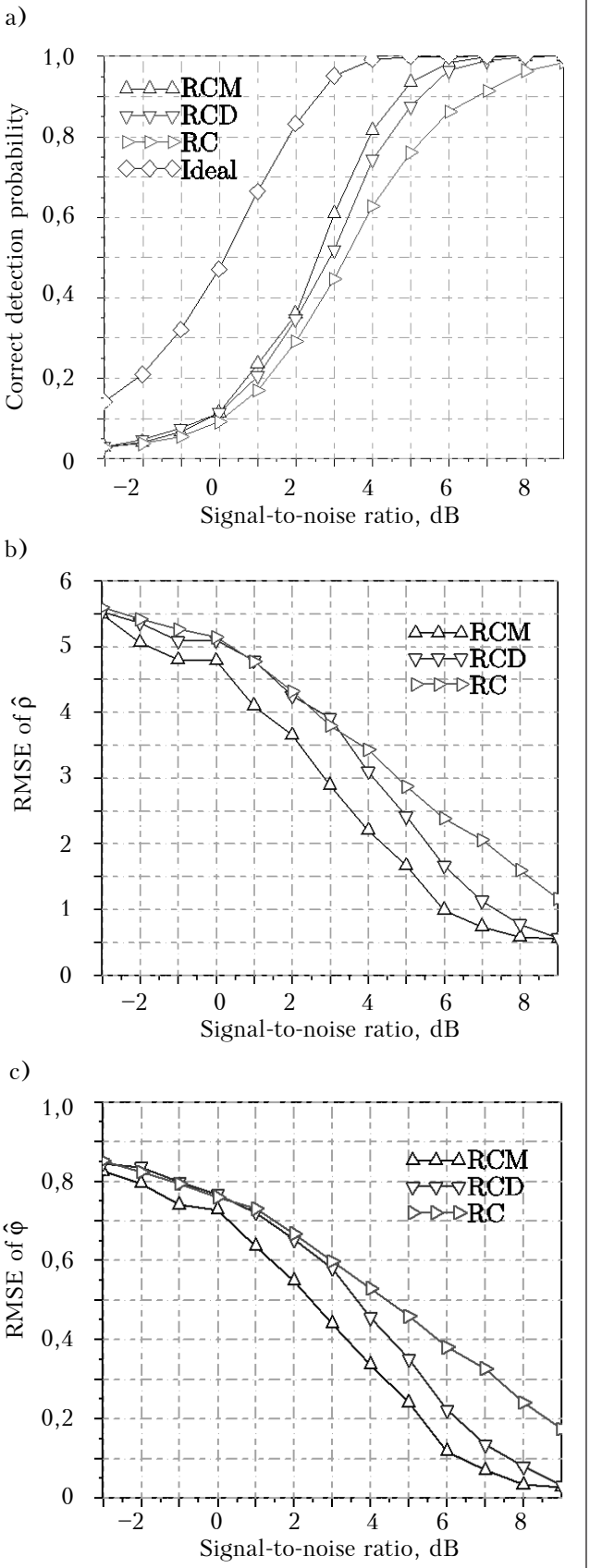

Fig. 14. Detection characteristics (*a*) and parameters estimation errors (*b*, *c*) with introducing the clearing procedure for different sample selection techniques

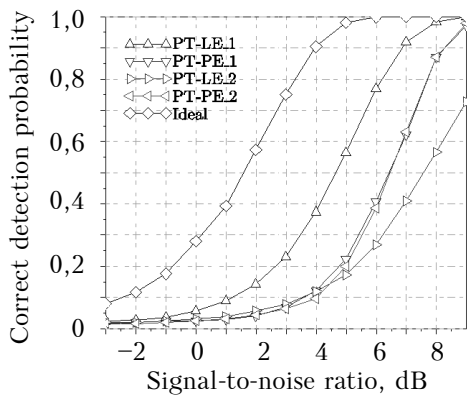

Fig. 15. Detection characteristics for parabolic trajectories

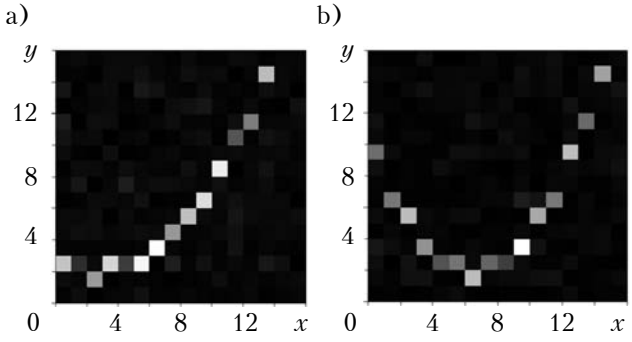

Fig. 16. Images with parabolic trajectories for **A**=[0.1, −0.6, 1.9] (*a*) and for **A**=[0.2, −2.8, 10.8] (*b*)

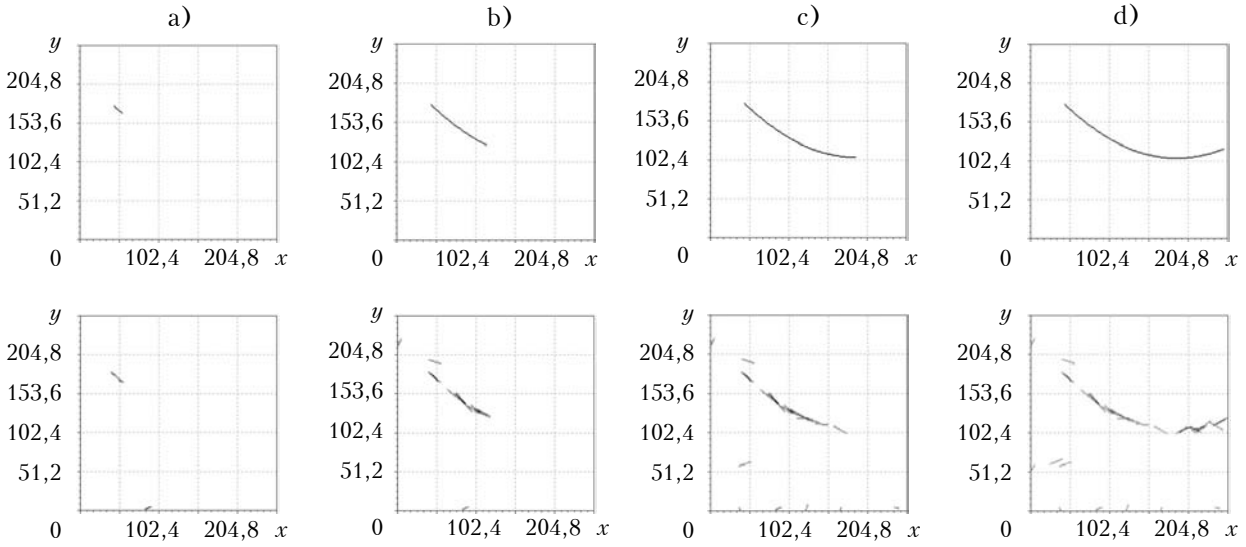

Fig. 17. True trajectories (top) and estimated local trajectories (bottom) of moving target at time step 1 (*a*), 6 (*b*), 12 (*c*) and 17 (*d*) at SNR = 9 dB

Target moves through observed region in a parabolic trajectory. At every scan all radar subplots are analyzed. Local trajectory paths, for which value of (11) exceeds threshold (which can be fixed or adaptive), are joined to previously obtained results to build the full trajectory. The task of further cancellation of false local paths should then be solved. This task is not considered in this paper and can be solved, for example, by any of classical algorithms of secondary radar signal processing [25].

Conclusion

It was shown that usage of Gaussian kernel smoothing as the preprocessing step can give some gain in target detection performance and accuracy of the estimation of trajectory parameters.

The additional clearing procedure for reducing false important samples can gives about 1 dB gain in target detection performance (with probability of correct detection 0,9) and increases accuracy of estimation of the trajectory parameters for SNR>0 dB.

In general, the proposed algorithm loses to an optimal algorithm for detection of targets with known trajectory about 3 dB in a threshold signal with the probability of correct detection 0,9 and probability of false alarms 0,01.

The proposed algorithm can be used in radars for detection and local trajectory parameters estimation of moving radar objects. Such local trajectory paths can then be used to build full trajectory of a target. Another field of use of this algorithm can be the tasks of radar meteor detection and analysis of visual or infrared images (e.g. FLIR images). It can also be used for forming more precisely proposed distributions in some PF TBD approaches, or as initiation procedure for complex trajectory detection by analysis of its small linear part.

REFERENCES

1. Li X. R., Bar-Shalom Y. Multiple-model estimation with variable structure. *IEEE Trans. Autom. Control*, 1996.— vol. 41, no 4, pp. 478-492.

2. Ristic B., Arulampalam S., Gordon N. *Beyond the Kalman Filter: Particle Filters for Tracking Applications*, Artech House, 2004.

3. Viterbi A. J. Error bounds for convolutional codes and an asymptotically optimum decoding algorithm. *IEEE Trans. Inf. Theory*, 1967, vol. 13, no 2, pp. 260-269.

4. Jang B., Rabiner L. An introduction to hidden Markov models. *IEEE ASSP Mag*, 1986, vol. 3, no 1, pp. 4-16.

5. Pohlig S. C. An algorithm for detection of moving optical targets. *IEEE Trans. Aerosp. Electron. Syst*, 1989, vol. 25, no 1, pp. 56–63.

6. Bruno M. G. S., Moura J. M. F. Multiframe detector/tracker: Optimal performance. *IEEE Trans. Aerosp. Electron. Syst*, 2001, vol. 37, no 3, pp. 925-945.

7. Tonissen S. M., Bar-Shalom Y. Maximum likelihood track-before-detect with fluctuating target amplitude. *IEEE Trans. Aerosp. Electron. Syst*, 1998, vol. 34, no 3, pp. 796-809.

8. Salmond D. J., Birch H. A particle filter for track-before-detect. *Proc. of the American Control Conf*, USA, VA, Arlington, 2001, pp. 3755–3760.

9. Driessen H., Boers, Y. Efficient particle filter for jump Markov nonlinear systems. *Radar, Sonar and Navigation, IEE Proceedings*, 2005, vol. 152, no 5, pp. 323-326.

10. Rutten M. G., Gordon N. J., Maskell S. Recursive track-before-detect with target amplitude fluctuations. *IEE Proc. Radar, Sonar and Navigation*, 2005, vol. 152, no 5, pp. 345-352.

11. Rutten M. G., Gordon N. J., Maskell S. Efficient particle-based track-before-detect in Rayleigh noise. *Proc. of the 7th Int. Conf. on Information Fusion*, Sweden, Stockholm, 2004, pp. 693-700.

12. Streit R. L., Graham M. L., Walsh M. J. Multitarget tracking of distributed targets using histogram-PMHT. *Digital Signal Processing*, 2002, vol. 12, no 2-3, pp. 394-404.

13. Blanding W. R., Willett P. K., Bar-Shalom Y. Off-line and real-time methods for ML-PDA track validation. *IEEE Trans. Signal Process*, 2007, vol. 55, no 5, pp. 1994–2006.

14. Kirubarajan T., Bar-Shalom Y. Low observable target motion analysis using amplitude information. *IEEE Trans. Aerosp. Electron. Syst*, 1996, vol. 32, no 4, pp. 1367-1384.

15. Stone L. D., Barlow C. A., Corwin T. *Bayesian Multiple Target Tracking*, Norwood, MA: Artech House, 1999.

16. Colegrove S. B., Davis A. W., Ayliffe J. K. Track initiation and nearest neighbours incorporated into probabilistic data association. *Journal of Electrical and Electronics Engineers, Australia*, 1986, vol. 6, no 3, pp. 191-198.

17. Davey S. J., Gray D. A. Integrated track maintenance for the pmht via the hysteresis model. *IEEE Trans. Aerosp. Electron. Syst*, 2007, vol. 43, no 1, pp. 93–111.

18. Davey S. J., Rutten M. G., Cheung B. A comparison of detection performance for several Track-Before-Detect algorithms. *Proc of the 11th Int. Conf. on Information Fusion*, Germany, Cologne, 2008, pp. 1-8.

19. Leite E., Alves G., Seixas J. et al. Radar meteor detection: concept, data acquisition and online triggering. In Book: Wave Propagation. Ed. by Dr. Andrey Petrin, InTech, 2011, pp. 537-549. http://www.intechopen.com/books/wave-propagation/radar-meteor-detection-concept-data-acquisition-and-online-triggering.

20. Yilmaz A., Shafique K., Shah M. Target tracking in airborne forward looking infrared imagery. *Proc. Image Vision Comput*, 2003, vol. 21, no 7, pp. 623-635.

21. Саваневич В. Е., Брюховецкий А. Б., Кожухов А. М., Диков Е. Н. Метод обнаружения астероидов, основанный на накоплении сигналов вдоль траекторий с неизвестными параметрами. *Системи оброб. інформації*.: Зб. наук. праць. Харків. 2011. Вип. 2. С. 137-144. [Savanevich V. E., Kozhuhov A. M., Briuhovetskii A. B. et al. *Systemy obrobky informatsii: Zb. nauk. prats. HUPS*, Kharkiv, 2011, no 92(2), pp. 137-144 (in Ukrainian)]

22. Prokopenko I., Vovk V., Omelchuk I., Chirka Y. Tracking and detection of rapid moving targets. *Proc. of the 14th International Radar Symposium (IRS)*, Germany, Dresden, 2013, vol. 2, pp. 768-773.

23. Chernov N., Lesort C. Least squares fitting of circles and lines, 2003. http://arxiv.org/abs/cs/0301001v1

24. Duda R. O., Hart P. E. Use of the Hough transformation to detect lines and curves in pictures. *Comm. ACM*, 1972, vol. 15, pp. 11-15.

25. Кузьмин С. З. *Основы теории цифровой обработки радиолокационной информации*. Москва. Советское радио, 1974. [Kuzmin S. Z. Fundamentals of the theory of digital radar data processing. Moscow, Sovetskoie radio, 1974 (in Russian)]

26. Hart P. E. How the Hough transform was invented [DSP History]. *IEEE Signal Processing Mag*, 2009, vol. 26, no 6, pp. 18-22.

27. Ballard D. H. Generalizing the Hough transform to detect arbitrary shapes. *Pattern Recognition*, 1981, vol. 13, no 2, pp. 111-122.

28. Vassileva B. Target detection and track formation algorithm for radar management and tracking benchmark with ECM. *Reports of the Bulgarian Academy of Sciences*, 2001, vol. 54, no 5, pp. 35-38.

29. Fardi B., Wanielik G. Hough transformation based approach for road border detection in infrared images. *Intelligent Vehicles Symp., 2004 IEEE*, Italy, Parma, 2004, pp. 549-554.

Дата поступления рукописи
в редакцию 30.09 2013 г.

І. Г. ПРОКОПЕНКО, В. Ю. ВОВК, І. П. ОМЕЛЬЧУК, Ю. Д. ЧИРКА, К. І. ПРОКОПЕНКО

Україна, м. Київ, Національний авіаційний університет
E-mail: prokop-igor@yandex.ru, vitalii.vovk@nau.edu.ua

ЛОКАЛЬНА ОЦІНКА ПАРАМЕТРІВ ТРАЄКТОРІЇ ТА ВИЯВЛЕННЯ РУХОМИХ ЦІЛЕЙ НА ФОНІ РЕЛЕЇВСЬКОЇ ЗАВАДИ

Розглянуто проблему та запропоновано алгоритм виявлення та локальної оцінки параметрів траєкторії рухомих цілей на основі аналізу даних у формі двовимірного зображення. Виходячи з прийнятих моделей цілі та детектора, фонова завада має розподіл Релея, а сигнал — розподіл Райса. Розглянуто два методи оцінки параметрів траєкторії: метод найменших квадратів і метод перетворення Хафа.

Запропоновано процедуру виявлення цілі, що ґрунтується на інтегруванні відбитої потужності вздовж імовірної траєкторії. Проведено статистичне моделювання, за результатам якого побудовано характеристики виявлення для запропонованого алгоритму.

Ключові слова: виявлення, стеження, рухомий об'єкт, оцінка параметрів, траєкторія, track-before-detect, розподіл Релея, перетворення Хафа, метод найменших квадратів.

И. Г. ПРОКОПЕНКО, В. Ю. ВОВК, И. П. ОМЕЛЬЧУК, Ю. Д. ЧИРКА, К. И. ПРОКОПЕНКО

Украина, г. Киев, Национальный авиационный университет
E-mail: prokop-igor@yandex.ru, vitalii.vovk@nau.edu.ua

ЛОКАЛЬНАЯ ОЦЕНКА ПАРАМЕТРОВ ТРАЕКТОРИИ И ОБНАРУЖЕНИЕ ДВУЖУЩИХСЯ ЦЕЛЕЙ НА ФОНЕ РЭЛЕЕВСКОЙ ПОМЕХИ

Рассмотрена проблема и предложен алгоритм обнаружения и локальной оценки параметров траектории движущихся целей на основе анализа данных в форме двумерного изображения. Исходя из принятых моделей цели и детектора, фоновая помеха имеет распределение Рэлея, а сигнал — распределение Райса. Рассмотрены два метода оценки параметров траектории: метод наименьших квадратов и метод преобразования Хафа. Предложена процедура обнаружения цели, основанная на интегрировании отраженной мощности вдоль вероятной траектории. Проведено статистическое моделирование, по результатам которого построены характеристики обнаружения для предложенного алгоритма.

Ключевые слова: обнаружение, слежение, движущийся объект, оценка параметров, траектория, track-before-detect, распределение Рэлея, преобразование Хафа, метод наименьших квадратов.

НОВЫЕ КНИГИ

Джиган В. И. Адаптивная фильтрация сигналов: теория и алгоритмы.— Москва: Техносфера, 2013.

В монографии рассматриваются основные разновидности адаптивных фильтров и их применение в радиотехнических системах и системах связи. Дано представление о математических объектах и методах, используемых в теории адаптивной фильтрации сигналов. Рассматриваются приемы получения вычислительных процедур, сами процедуры и свойства таких алгоритмов адаптивной фильтрации, как алгоритмы Ньютона и наискорейшего спуска, алгоритмы по критерию наименьшего квадрата, рекурсивные алгоритмы по критерию наименьших квадратов и их быстрые (вычислительно эффективные) версии; рекурсивные алгоритмы по критерию наименьших квадратов для многоканальных фильтров и их версии для обработки нестационарных сигналов, а также многоканальные алгоритмы аффинных проекций. Дано описание стандартных и нестандартных приложений для моделирования адаптивных фильтров на современных языках программирования MATLAB, LabVIEW и SystemVue, а также реализаций адаптивных фильтров на современных цифровых сигнальных процессорах отечественного и зарубежного производства. Особенностью материала является изложение теоретических материалов для наиболее общего случая — адаптивных фильтров с комплексными весовыми коэффициентами, наличие разделов по многоканальным адаптивным фильтрам и алгоритмам адаптивной фильтрации нестационарных сигналов. Книга является первым систематическим изложением теории адаптивной фильтрации на русском языке. Предназначена для научных работников, инженеров, аспирантов и студентов радиотехнических и связных специальностей, изучающих и использующих на практике цифровую обработку сигналов и, в частности, адаптивную фильтрацию сигналов.